Communicating the deadly consequences of global warming for human heat stress

Tom KR Matthews[1], Robert Wilby[2], Conor Murphy[3]

[1]Liverpool John Moores University, [2]Loughborough University, [3]National University of Ireland, Maynooth

Submitted to Proceedings of the National Academy of Sciences of the United States of America

In December 2015 the international community pledged to limit global warming to below 2°C above preindustrial (PI) to prevent *dangerous* climate change. However, to what extent, and for whom, is danger avoided if this ambitious target is realised? We address these questions by scrutinizing heat stress, because the frequency of extremely hot weather is expected to continue to rise in the approach to the 2°C limit. We use analogues and the extreme South Asian heat of 2015 as a focussing event to help interpret the increasing frequency of deadly heat under specified amounts of global warming. Using a large ensemble of climate models, our results confirm that global mean air temperature is non-linearly related to heat stress, meaning that the same future warming as realised to date could trigger larger increases in societal impacts than historically experienced. This non-linearity is higher for heat stress metrics that integrate the effect of rising humidity. We show that even in a climate held to 2°C above PI, Karachi (Pakistan) and Kolkata (India) could expect conditions equivalent to their deadly 2015 heatwaves *every year*. With only 1.5°C of global warming, twice as many megacities (such as Lagos, Nigeria and Shanghai, China) could become heat-stressed, exposing more than 350 million more people to deadly heat by 2050 under a mid-range population growth scenario. The results underscore that *even if* the ambitious Paris targets are realised, there could be a significant adaptation imperative for vulnerable urban populations.

Projected heat stress | Climate change mitigation targets | Deadly heat | Heat index | Climate change in megacities

Air temperatures near the surface of Earth are rising. At the time of writing, 2015 was the warmest year globally since observations began (Fig. 1A). Higher average air temperatures coincide with more frequent periods of extremely hot weather[1,2] which, in turn, have adverse consequences for human well-being and economic productivity[3,4,5]. The health impacts of rising air temperature are compounded by attendant increases in atmospheric water vapour[6], which reduces humans' ability to dissipate heat[7].

Apparent temperature[8] translates the humidity effect into an index that provides a "feels-like" temperature. Whilst far from the only metric of its type, it is amongst the most widely used to communicate episodes of extreme heat[9, 10]. For example, the United States National Weather Service (NWS) approximate *apparent temperature* with their Heat Index (HI) (See: Materials and methods). The NWS issue warnings when forecasted values persist above 105°F (with HI = 40.6°C; hereafter HI40.6) – an operational definition of "dangerous" heat. During 2015, annual maxima for HI were well above average across South Asia and around the Persian Gulf (Fig 1B), with extreme values above 60°C gaining widespread media attention[11]. Some heat-prone megacity regions such as Karachi (Pakistan) and Kolkata (India) recorded their highest HI values in at least 36 years (Fig 1 B-D). The extraordinary heat had deadly consequences, with over 3,400 fatalities reported across India and Pakistan alone[12].

In the context of a warming climate, occurrence of such extreme HI conditions should not be surprising. By definition, the HI has temperature sensitivity much greater than unity at high values (Fig S1). This is common to temperature-humidity heat stress indicators[13] because, for a given relative humidity, latent heat cooling capacity decreases at an accelerating rate in response to the rise in vapour pressure governed by the Clausius-Clapeyron relation. Without counteracting reductions in relative humidity, higher air temperatures drive yet greater increments in HI. This is underlined by Fig 2 which shows HI derived from the model integrations of the Coupled Model Inter-comparison Project Phase 5 (CMIP5)[14]. Comparing the decade 1979-1988 with 2090-2099, it is evident that extreme HI values (here defined as the 99.9th percentile) over land rise much faster in response to global mean air temperature increase than either mean or extreme air temperatures.

Given the threat *already* posed by heat stress worldwide[15] this temperature sensitivity is of significant concern. Projections of changes in heat stress have accordingly received attention from the research community[9, 10, 16]. For upper-bound, end of 21st Century warming, heat in some regions could exceed the physiological tolerance of humans[17], with presently rare heat thresholds being crossed far more regularly[16]. The frequency of hot extremes has also been observed to be highly sensitive to global mean temperature increase[2]. This is expected to drive increasing heat stress for little additional climate change[18], with even 2°C warming since PI considered unlikely to avoid an intensification of severe heat events[19].

Mindful of these impacts and sensitivity, we examine the extent to which the global warming limits of 1.5 and 2°C agreed in Paris by the international community[20] may avoid *dangerous* climate change from a heat-stress perspective. The issue is explored

Significance

Extremely hot weather can have deadly human consequences. As the climate warms, the frequency and intensity of such conditions is expected to increase – one of the most certain negative impacts expected under global warming. Concerns about dangerous climate change have spurred the international community to commit to limiting global temperature changes to below 2°C above pre-industrial. Whilst lauded as a great achievement to avoid *dangerous* climate change, we find that even if such aspirations are realised, large increases in the frequency of deadly heat should be expected, with more than 350 million more megacity inhabitants afflicted by mid-century. Such conclusions underline the critical role for ambitious adaptation to accompany these climate change mitigation targets.

Reserved for Publication Footnotes

Submission PDF

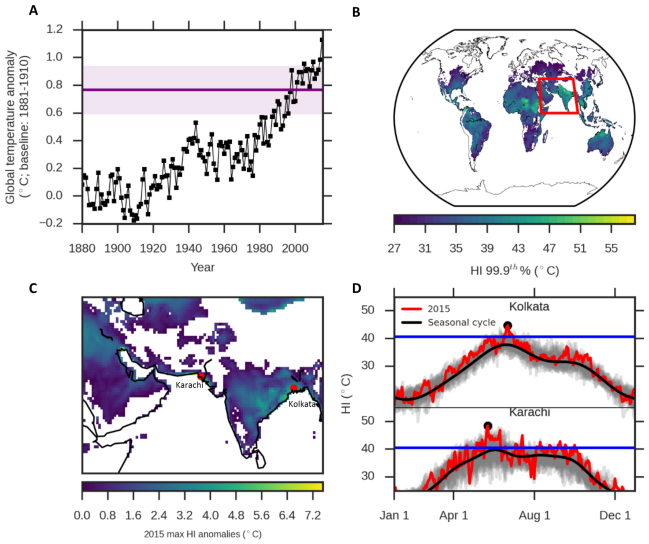

Fig. 1. Mean air temperatures and recent HI extremes. (A) Global mean air temperature series defined as the average of the BEST, HadCRUT4 and GISTEMP records. The purple line gives the 1986-2015 mean, with shaded area representing ± one standard deviation. (B) 99.9th percentiles of daily HI values, with values <27°C masked (the lower limit of the HI warning category indicating "caution" to heat stress). (C) HI anomaly of 2015 relative to the mean of the annual maximums 1979-2015; negative anomalies are masked, as are positive anomalies where absolute HI <27°C. Note that the domain of (C) is indicated in (B) by the red box. (D) Daily mean HI values for the respective regions (1979-2015). Grey curves are individual years 1979-2014, red is 2015.

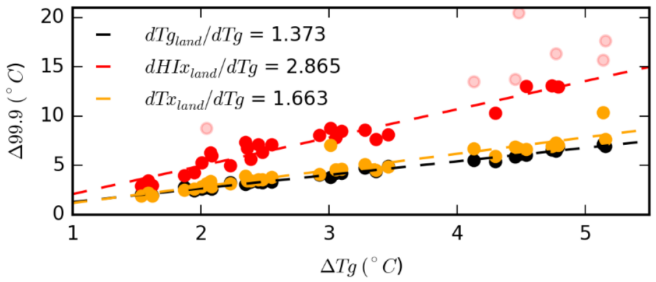

Fig. 2. Relationship between CMIP5 modelled changes in global mean air temperature (ΔTg) and changes in: mean air temperature over land (Tg_{land}), extreme temperatures over land (Tx_{land}), and HI values over land (HIx_{land}). Extremes are defined as the 99.9th percentile, and the changes are calculated by differencing the respective values in the last decade of model simulations (2090-2099) relative to the simulated values over the period 1979-1988. Note that we mask HI values >50°C when computing the regression slope (shown in lighter shading), as this is the upper-limit of the range considered by ref 8.

by assessing heat stress projections as a function of global temperature change. This approach has been applied elsewhere in climate impacts research and permits quantification of sensitivity across a range of policy-relevant warming targets[21,22,23]. We also employ temporal and spatial analogues to facilitate communication of these results to the wider public. The use of analogues assume that conditions already experienced may present similar challenges when manifesting elsewhere or in the future and have been used widely by the climate research community[24]. The allure of analogues stems from their potential to educate a wide range of non-specialists about the complex impacts of climate change, providing a first step to comprehending the unknown[25].

An emphasis on communication is necessary because warming consistent with the Paris targets has been described as sound-

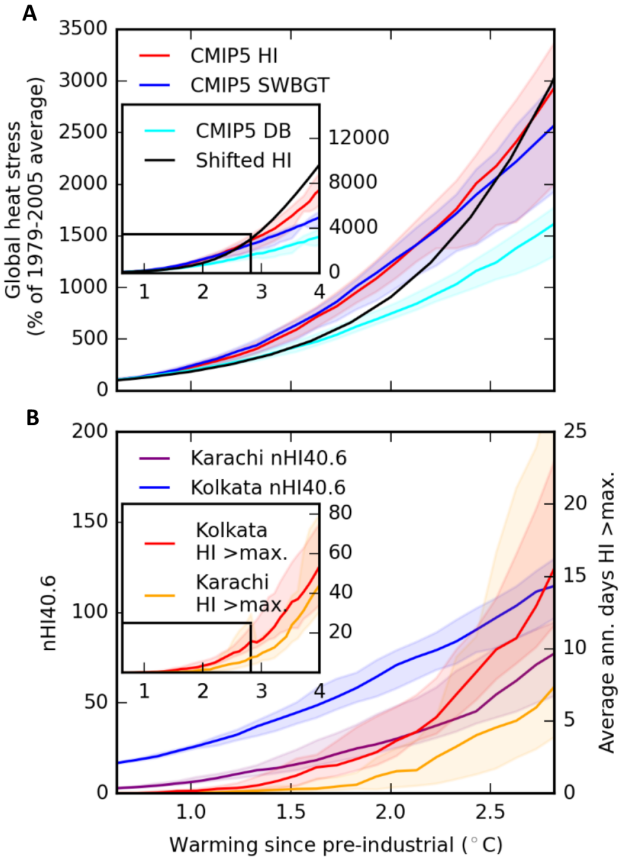

Fig. 3. Global and regional heat stress projected as a function of global warming amounts. (A) Global (land) heat stress sensitivity to global air temperature changes, in which lines are medians calculated from the CMIP5 ensemble and the shaded region spans the 25th-75th percentiles. Note that heat stress is defined here as the mean annual number of days exceeding a threshold temperature (40.6, 35 and 37.6°C for the HI, SWBGT, and DB temperatures, respectively). At this global-scale, these metrics are area-averaged. Inset plot (A) continues the curves to 4°C warming above pre-industrial, with limits in the main plot indicated by the black box. (B) As in (A) but for the named locations, with different units on the y-axes. Series on inset axes continue the respective curves from the main plot to 4°C.

ing modest enough for the urgency of the situation to be lost on non-experts[26]. Such interpretation may downplay the risk of climate change, which in turn could make individuals less willing to take action to reduce climate change[27]. In reality, the period 1986-2015 was approximately 0.8°C above PI (here defined as 1881-1910; Fig 1A). Hence, the 1.5 and 2°C Paris targets allow for only a further 0.7 and 1.2°C warming [although a global mean temperature rise of 2.7°C is expected under the current set of Intended Nationally Determined Contributions (INDCs)]. In other words, the ambitious targets still commit to between 1.9 and 3.4 times the warming already experienced since the Industrial Revolution, which in turn propagates into much greater changes in the severity of extreme HI conditions (Fig 2). Our analysis highlights combined temperature-humidity heat stress impacts as a reason for concern, and draws upon analogues to illustrate the challenges that may be ahead.

First, we show the global-scale sensitivity of HI in terms of threshold exceedances (Fig 3A). Sliding 30-year samples of changes in global mean temperature since 1881-1910 from transient CMIP5 simulations are plotted against concurrent changes in bias-corrected global heat stress (defined here as the area-weighted average number of days with mean HI above HI40.6 [nHI40.6]). The relationship between the global heat stress bur-

submitted

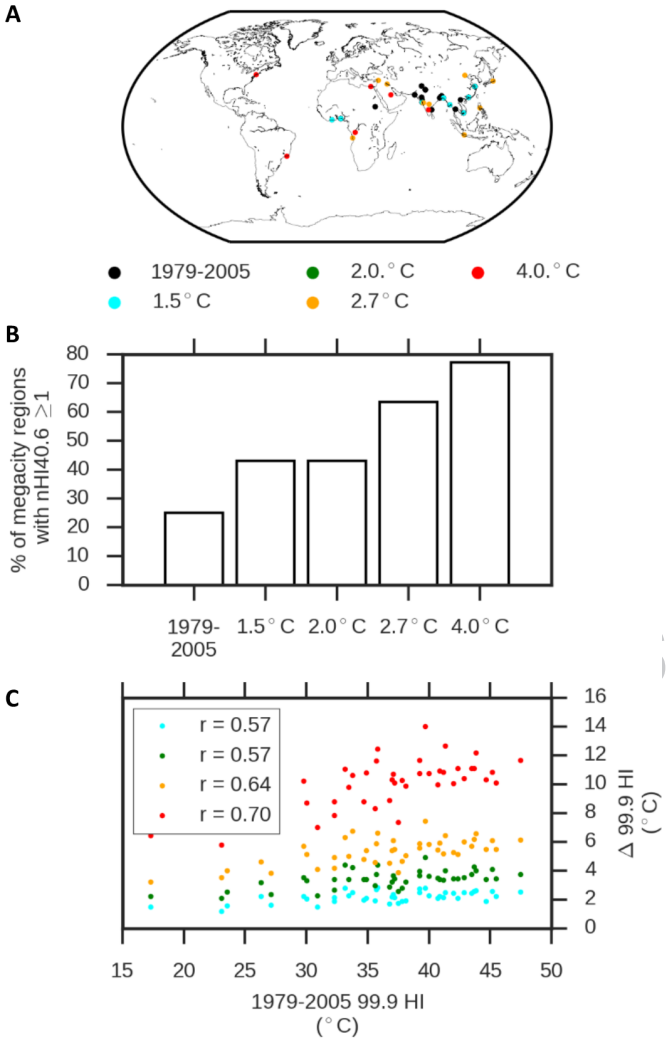

Fig. 4. Changes in heat stress for global city regions under various scenarios of global warming. (A) City regions experiencing annual heat stress (nHI40.6 ≥1) for the first time under different warming amounts according to the CMIP5 ensemble median. Black circles mark locations already experiencing heat stress during the 1979-2005 reference period. Note that the names of these cities are available in SI tables 2-5. (B) CMIP5 ensemble median percentage of megacities experiencing common heat stress under the respective warming amounts. (C) Changes in the CMIP5 ensemble median 99.9th HI percentile as a function of the observed 99.9th HI percentile during the 1979-2005 reference period. Values for HI >50°C have been masked out of this plot and the inset correlations (see Fig. 2 caption).These correlations (r values) quantify the strength of the positive relationship plotted. Note that the critical r value for rejection of the null hypothesis (r=0) is +/-0.30 for 42 degrees of freedom, at the 0.05 level, hence all reported values are interpreted as significant.

den and global mean air temperature exhibits non-linearity that is robust to variants of our method, with higher heat-stress sensitivity under increasing temperatures also evident when (i) threshold exceedances of 35°C Simplified Wet Bulb Globe Temperature (SWBGT) are used (another common heat stress metric[5]); and (ii) the transient CMIP5 projections are replaced by pattern-scaled temperature observations and fixed relative humidity (see SI Section 4). Notably, the frequency of extreme values increases slower for a reference dry-bulb (DB) temperature of 37.6°C (with equivalent rarity to HI40.6 during the 1979-2005 observational record) as the climate warms. Hence, assessments based on sensitivity of heat extremes' frequency to global temperature change through DB[2] should be regarded as conservative projections of human heat stress.

Fig S2provides more detail of these changes, highlighting that, as global air temperatures rise, the land area experiencing dangerous HI values increases, with pole-ward expansion particularly evident in the Northern Hemisphere. The frequency of dangerous HI values also increases for those regions that are already impacted. The combined effect of increased area and frequency explains why global heat stress should be expected to follow a non-linear relationship with global mean air temperature over the range considered here. With the area-weighted mean heat stress defined as $A\bar{N}$ (where A is the fraction of the Earth's land surface experiencing dangerous HI, and $\bar{N}$ is the area-weighted mean number of days experienced within this region), non-linearity will result if both terms are a function of global air temperature (as evident from the product rule of calculus). The practical implication of this relationship is that societies will be disproportionately impacted by heat stress as global temperature increases. Larger populations will be exposed to dangerous HI values, and those already affected will be subjected to harmful conditions more often and with greater severity.

This non-linearity also means that any change in global heat stress burden experienced from warming to date will be smaller compared with the same additional warming realised in the future. This has two implications. First, vulnerable communities may be insufficiently prepared to manage a non-linear growth in extreme heat risk[28]. Second, there could be progressively heavier impacts if the Paris warming targets are missed. For example, according to the median CMIP5 HI curve in Fig 3A, under 1.5°C global warming, the heat stress burden will be 5.7 times that experienced during the reference period (1979-2005). This rises to between ~12 and 26 times the reference heat stress under 2 and 2.7°C warming, respectively. The avoided impacts of mitigation are shown in the inset of Figure 3A by continuing the curves in the main plot to 4°C of global warming. Under these temperatures, CMIP5 HI reaches more than 75 times the reference value for $A\bar{N}$.

The possible consequences of these projections can be made more tangible by employing the recent heatwaves of Karachi and Kolkata as analogues. Since HI40.6 is already expected each year at these locations, likely resulting in some degree of acclimatisation[29], we show in Fig. 3B counts of annual exceedance of the historical maximum daily mean HI on record alongside HI40.6. The results indicate that HI values in excess of the deadly record set in 2015 would become common place in the absence of mitigation efforts (inset Fig 3B), with more than 40 (50) days a^{-1} expected in Karachi (Kolkata) under global warming of 4°C. Whilst effects are much reduced if warming is limited to levels consistent with the INDCs or the 1.5 and 2°C targets, we highlight that there will likely be significantly increased heat stress, even if mitigation does successfully hold global warming to the ambitious 1.5°C target. According to the ensemble median, a global warming of 1.5°C would imply that Kolkata experiences, on average, conditions equivalent to the 2015 record every year; Karachi would experience the same deadly heat about once every 3.6 years. Under 2°C of global warming, both regions could expect such heat on an annual basis. The potential societal impacts of extreme heat are well documented[3, 4] and some of these were manifested in Karachi and Kolkata during 2015. Conservative estimates suggest that there were 1,200 heat-related deaths in Karachi, and enhanced mortality and economic disruption in Kolkata[30, 31]. In this context, the projections of Fig 3B are evidently of significant concern.

We explore the broader potential societal impacts of global warming on heat stress by examining projections for other megacity regions. These were identified according to the 21st Century population projections from ref 32, focussing on cities within the top 101 by population size for all three Shared Socioeconomic Pathways (SSPs)[33] and all time-slices considered by the authors (2010-2100; see Materials and methods). Our subset of 44 cities

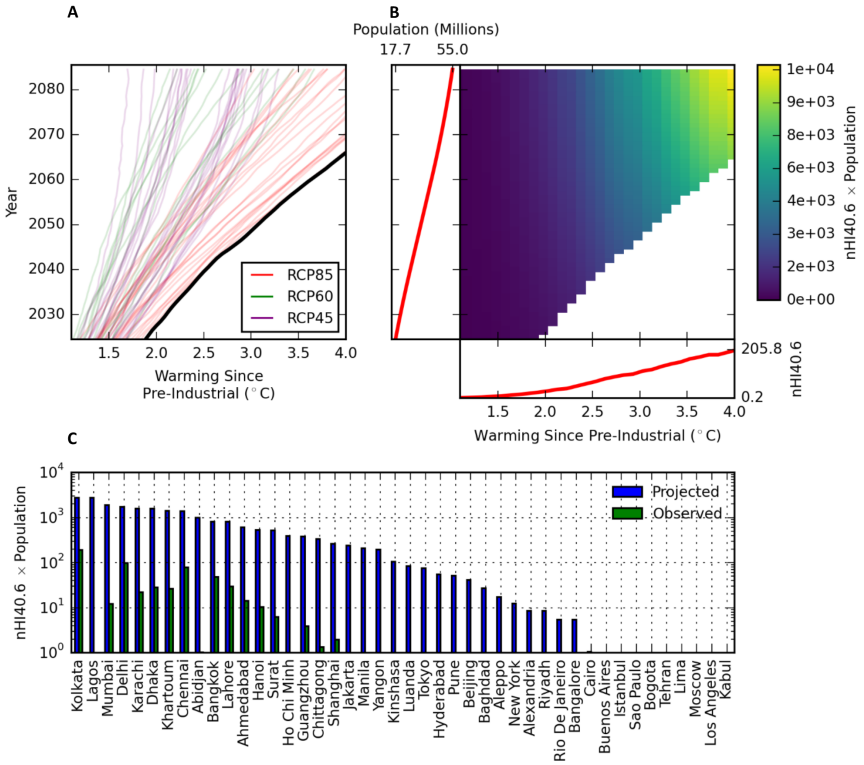

Fig. 5. Population-weighted heat stress throughout the 21st Century. (A) Running 30-year means of CMIP5 warming since pre-industrial. The fastest warming series is plotted with a heavy (black) line. Warming rates in excess of this are masked in panel B, which shows an example (for Lagos [Nigeria], under SSP2) of the ensemble-median for all other combinations of global warming amounts and running 30-year population averages; the small inset panels attached to the respective axes show the evolution of the respective variables that are multiplied together to form the matrix. (C) The mean projected over the 21st Century across all SSP matrices for the respective cities. The reference is computed using HI values for 1979-2005 along with the 1995 population estimate; see Materials and methods for details of these calculations.

accounts for 0.4 billion people in 2010, and is projected to reach between 0.94 and 1.1 billion by 2100 depending on the SSP. For each of these megacities we identified under which warming scenarios they may begin to experience heat stress annually [using the criteria from the CMIP5 ensemble median projection of nHI40.6 ≥ 1; see SI Section 3 for full information of this city-level assessment, including detailed projections for those locations becoming heat stressed (SI tables 2-5)]. We also show in SI tables 2-5, the historical spatial analogues (megacities) that best match the conditions (nHI40.6, and values of the HI 99.9th percentiles) in cities projected to become newly heat-stressed.

Fig 4A indicates that with 1.5°C of global warming a number of city regions in West Africa and South/East Asia can expect to experience heat stress for the first time. Lagos (Nigeria), for example, would be newly heat stressed according to our definition and could expect nHI40.6 similar to that endured by Delhi (India) during the reference climate of 1979-2005. The closest historical analogue for Shanghai (China) – also newly heat stressed – would be Karachi. Globally, over 40% of these 44 largest cities would be annually heat stressed for a warming of 1.5°C (Fig 4B), representing a doubling relative to the reference period. With temperatures 2°C above PI, no additions are made to the list of newly heat stressed cities, but that reflects the spatial distribution of our sampled locations. Under even higher temperature change scenarios, new cities annually experiencing heat stress continue to emerge. For the INDC level of 2.7°C warming, for example, the largest city in the world at present (Tokyo, Japan), and the Chinese megacity of Beijing could be among those affected. With 4.0°C warming, nearly 80% of the 44 megacities could be annually heat stressed, including New York and Rio de Janeiro.

Fig 4C suggests that those cities already accustomed to extreme heat can expect larger increases in extreme HI values under the respective warming scenarios (consistent with Figure 2). Use of these city exemplars reinforces the point that for progressively higher warming amounts, not only will heat stress spread to new populations, but that those already exposed will be challenged by the largest increases in HI intensity.

The heat stress threat posed by climate change is accentuated by assumed population growth over the coming century. To explore the combined effect of warming and population change in these 44 cities, we defined a population-weighted Heat Stress Burden (*HSB*) as the CMIP5 ensemble median nHI40.6, multiplied by the population for each city. By computing the metric using HI projections for different amounts of global warming, combined with population projections for a plausible range of years (see Fig 5A), we provide insight into the possible effects of specified climates prevailing during particular time periods (Fig. 5B). By averaging over all combinations (of years/warming amounts) and SSPs, we can then rank the cities according to their projected *HSB* over the 21st Century (Fig. 5C; See Materials and methods for more details of this procedure). Note that our method yields insight into conditions beyond the range of specific Representative Concentration Pathways (RCPs) driving the CMIP5 ensemble. For example, the time-evolving impact of stabilising temperatures at 1.5°C above PI can be assessed (by simply reading the relevant x-coordinate in Fig. 5B).

This analysis suggests that South Asian cities will remain the most heat stressed over the coming century, as six out of the top ten by *HSB* are located in Pakistan, India or Bangladesh. African cities also feature prominently, with Lagos (Nigeria), Abidjan (Ivory Coast), and Khartoum (Sudan) taking three of the remaining four spots in the top ten. Notably, Lagos and Abdijan are also projected to realize some of the largest relative *changes* in heat stress burden (the largest and third-largest, respectively; Ho Chi Minh is projected to experience the second-largest change), which is due to a combination of rapid population growth and sharp increases in nHI40.6. For example, under 1.5°C warming, the CMIP5 ensemble median projects that Lagos could see a 106-fold increase in nHI40.6 relative to 1979-2005; under SSP2, population in Lagos peaks during 2070-2099 with an 11-fold increase relative to 1995. A 1.5°C warmer climate at the end of

this century would therefore result in a HSB more than a thousand times greater than the recent past for Lagos. Across all megacities we estimate that, with this level of warming under SSP2, and as early as the middle of the 21st Century, more than 350 million more people (a four-fold increase) could be exposed to heat stress annually compared to the 1979-2005 reference period.

In summary, we emphasise that the potentially deadly consequences of heat stress linked to global warming, even if limited to the 1.5°C Paris target, should not be overlooked. More of the Earth's land surface could experience dangerous heat, and those already exposed could encounter such conditions more often. Whilst the challenge of reaching a universal definition of 'dangerous' heat are acknowledged – in terms of metric, timing, and duration – the fact remains that conditions that have historically challenged (and overwhelmed) those living in some of the most heat-stressed regions on Earth, could become much more frequent. Population growth in vulnerable regions will add to the challenge. We used megacities to quantify the impacts of these combined climate and societal pressures, but acknowledge that the spatially-coarse climate models employed cannot resolve the specific city-scale microclimates[34] in detail. Nonetheless, we consider it unlikely that projections for cities are overly pessimistic, given that heat stress amplification associated with global warming is believed to be no less severe in urban environments[35]. Indeed, our frequency-based analysis of heat stress likely provides a conservative perspective on projected heat stress. We have also shown that regions characterised by historically higher HI extremes can anticipate larger increases in the HI with global temperature rise, meaning more *intense* heat stress could also result as the 40.6°C threshold is exceeded by greater amounts.

The high sensitivity to global temperature rise translates into a further doubling of global heat stress moving from 1.5°C to 2°C above PI (5.7 and ~12 times greater than 1979-2005, respectively), which, from a human health perspective, provides a strong incentive for limiting global warming to the lower of these targets. However, with a possible 350 million more people exposed to deadly heat by the middle of the century even if this target is met, our analysis shows the critical role for adaptation, alongside mitigation, to manage the potential societal impacts. In this aspect, urban centres, including the megacities used here to communicate projected heat stress, are recognized as key focal points for action on mitigating *and* adapting to climate change[36]. Some city authorities are already taking steps to limit the effects of extreme heat. For instance, Ahmadabad (India) recently implemented South Asia's first comprehensive heat action plan, which may soon be expanded across the region[37]. Given the dual pressures of climate change and population growth on heat stress identified here, we foresee a need for such plans to be adopted more widely across vulnerable regions.

Materials and methods

Heat Index and climate model simulations

The National Weather Service (NWS) Heat Index (HI) was calculated using the algorithm of ref 38. The index was evaluated using daily mean modelled fields from the Coupled Model Inter-comparison Project Phase 5 (CMIP5) for the period 1979-2099, obtained through the Earth System Grid Federation (see Table S1 for an inventory of the runs employed). Model experiments from 2006 onwards reflect the Representative Concentration Pathways (RCPs); results for 1979-2005 were taken from the RCPs' constituent "historical" model runs, identified and spliced using available metadata. HI computation requires values of air temperature and relative humidity. The former was available directly from the CMIP5 archive, whilst relative humidity (RH) was derived from specific humidity and surface pressure (P_s):

$$RH = \frac{q P_s}{\varepsilon\, e_0 \exp\left[\frac{L}{R}\left(\frac{1}{T_0} - \frac{1}{T}\right)\right]} \times 100$$

Eq. 1

where q is specific humidity (g/g), ε is the ratio of gas constants for water vapour and dry air (0.622 $g_{vapour}/g_{dry\ .air}$), e_0 is 610.8 Pa, $\frac{L}{R}$ is 5423 K (latent heat of vaporization divided by the gas constant for water vapour), T_0 is 273.15 K, and T is the air temperature (K). P_s is not directly available and was calculated from the hypsometric equation, using mean sea level pressure, air temperature, and surface elevation. These CMIP5 HI values were calculated on native grids for each model, before being bi-linearly interpolated to the 0.5°×0.5° observational grid for bias-correction and subsequent analysis (see below for details of the observations, and SI Section 2 for information on the bias corrections).

To explore sensitivity of global heat stress projections to choice of heat stress metric (see Fig 3A), the Simplified Wet Bulb Globe Temperature (SWBGT) was also computed. This required air temperature and vapour pressure. Vapour pressure was obtained from the relative humidity by multiplying Eq. 1 by $e_0 \exp\left[\frac{L}{R}\left(\frac{1}{T_0} - \frac{1}{T}\right)\right]/100$.

In Fig 3A we also showed how the frequency of extreme dry-bulb (DB) temperatures (a value ≥ 37.6°C) responds to global warming in the CMIP5 ensemble. The threshold 37.6°C was chosen as we identified that this value had the same non-exceedance probability (99.95%) as a HI value of 40.6°C in the concurrent observational dataset (see below for details of the observations)

Heat Index and observations

For observations, the Watch-Forcing-Data-ERA-Interim (WFDEI) meteorological dataset[39] (1979-2014) was utilized. As with the CMIP5 data, HI and SWBGT values were calculated from daily mean air temperature and specific humidity; surface pressure was however available directly, eliminating the need for hypsometric adjustment. To place conditions in South Asia during 2015 into context (Fig 1C), observed HI values were bridged to this year using data from the ECMWF Interim Reanalysis[40] interpolated to the 0.5°× 0.5° WFDEI grid, through a point-by-point regression. The required linear functions were calibrated on the overlapping 1979-2014 data and forced with ECMWF data in 2015.

For the megacities of Karachi and Kolkata (Fig 1 D), HI values from the WFDEI data were similarly extended via regression, but both series (ECMWF and WFDEI) were first interpolated to their respective coordinates (Karachi: 24.86°N, 67.01°E; Kolkata: 22.57°N, 88.36°E). The amount of explained variance (r^2) for these city-specific regressions exceeded 0.95. Note that ERA-Interim HI values were calculated analogously for the WFDEI data with the exception that relative humidity first had to be calculated from dew-point air temperature. Full details of how projections were generated for the specific city regions are provided in SI sections 2 and 3.

Heat stress as a function of air temperature changes

To assess sensitivity of heat stress to global mean air temperature changes, the daily exceedances of HI40.6 computed from each CMIP5 ensemble member at each grid point were first summed annually, and then averaged spatially (accounting for grid-cell area) to produce series of the global-mean number of days above HI40.6. These series were then averaged over running 30-year periods (yielding nHI40.6). Over the same 30-year intervals, temperature changes since pre-industrial in the corresponding CMIP5 model runs were calculated by a) calculating the model-simulated difference relative to 1979-2005, and b) adding the observed warming experienced 1979-2005 relative to 1881-1910 to this amount. The observed warming 1979-2005 (0.63°C) was calculated as the average across the ensemble median of HadCRUT4[41], BEST[42], and GISTEMP[43]. To prepare Fig 3, statistics were calculated by linearly interpolating the global mean air temperature (the x-values) *vs.* heat stress (the y-values) relationship to a regular spacing of 0.1°C for each model run, and then calculating median and percentile statistics across this interpolated array.

Where the heat stress impacts associated with a given warming scenario are shown (Fig 4 and the accompanying text), heat stress conditions were sampled for simulated 30-year climates matching the given global warming amount most closely. We specified that the simulated global mean temperature had to be within an arbitrary tolerance of ±0.075°C to be considered representative of the specified warming scenario, and hence included in the ensemble statistics.

Population-weighted heat stress

To assess the combined effects of population growth and global warming on city-level heat stress throughout the 21st Century, we employed projections from ref 32, available for three SSPs and years: 2010, 2025, 2050, 2075, and 2100. We focussed on those (44) cities that remained in the top 101 for each of these time slices across the three SSPs. Projections for these cities were then linearly interpolated to annual resolution (2010-2099). We also obtained the 1995 population for each city from ref [44] to compute the reference heat stress burden (HSB) over the period 1979-2005. These burdens were calculated by multiplying nHI40.6 for a specified warming amount for each city ($nHI40.6_{City}$) by the respective population (P_{City}). The term $nHI40.6_{City}$ was computed as a function of global warming amounts in 0.1°C increments analogously to the global-scale metrics (see Heat stress as a function of air temperature changes), but without the spatial-averaging step. The ensemble median $nHI40.6_{City}$ was then multiplied by all possible running 30-year population averages for each city, giving insight into the heat stress

Submission Draft

burden for a wide range of scenarios. We masked combinations of warming amounts (which controls $nHI40.6_{City}$) and years that required faster rates of warming than the maximum recorded across the CMIP5 ensemble (see Fig 5c). The average 21st Century heat stress burden for each SSP was therefore calculated from:

$$HSB_{City,SSP} = \frac{1}{\sum H(T_g,i,j)} \sum_i \sum_j nHI40.6_{City_i} \times P_{City_j} \times H(T_g,i,j)$$

where the subscripts i and j index the global warming amounts and years, respectively; $H(T_g,i,j)$ is a Heaviside function that evaluates to one (zero) if the warming amount i is less (more) than the maximum CMIP5 global warming (T_g) for the 30-year period j. Averaging $HSB_{City,SSP}$ across the three SSPs yields the 21st Century heat stress burden plotted in Fig. 5C. Reference HSB was calculated by multiplying the observed (1979-2005) $nHI40.6_{City}$ by the 1995 population.

In the main text we also cite the number of megacity inhabitants with ensemble median nHI40.6 ≥ 1 for a +1.5°C climate ($n_{1.5}$), which was computed:

$$n_{1.5} = \sum_{City} H(nHI40.6_{City}, 1.5°C) \times P_{City,2050}$$

Where the Heaviside function evaluates to one (zero) if nHI40.6 for the respective $City$ is ≥ 1. $P_{City,2050}$ denotes the 30-year mean population projection (according to SSP2for this location and the 30-year period centred on 2050.

Data and code availability

The CMIP5 data underpinning our analysis can be downloaded from any of the nodes of the Earth System Grid Federation (e.g. https://esgf-data.dkrz.de), whilst the observational (WFDEI) dataset is available via ftp from ftp.iiasa.ac.at. The HadCRU, GISS and BEST global air temperature series can be sourced from: https://crudata.uea.ac.uk/cru/data/temperature/, https://data.giss.nasa.gov/gistemp/ and http://berkeleyearth.org/data/, respectively. The SSP megacity population projections were obtained from the authors of ref 32, and the 1995 population from ref [44] are available at https://esa.un.org/unpd/wup/CD-ROM/ (file 12). All processed data and computer code used in the analysis are available from the authors upon request.

Acknowledgements

TM thanks Daniel Hoornweg and Michelle Cloak for their help in accessing the city-level population projections. The anonymous reviewers are thanked for their thoughtful feedback.

1. Hansen J, Sato M, Ruedy R (2012) Perception of climate change. *Proc Natl Acad Sci USA* 109(37):E2415-E2423.
2. Fischer EM, Knutti R (2015) Anthropogenic contribution to global occurrence of heavy-precipitation and high-temperature extremes. *Nat Clim Chang* 5(6):560–564.
3. Sheridan SC, Allen MJ (2015) Changes in the Frequency and Intensity of Extreme Temperature Events and Human Health Concerns. *Curr Clim Chang Reports* 1(3):155–162.
4. Dunne JP, Stouffer RJ, John JG (2013) Reductions in labour capacity from heat stress under climate warming. *Nat Clim Chang* 3: 563-566.
5. Willett KM, Sherwood S (2012) Exceedance of heat index thresholds for 15 regions under a warming climate using the wet-bulb globe temperature. *Int J Climatol* 32(2):161–177.
6. Collins M, et al. (2013) Long-term Climate Change: Projections, Commitments and Irreversibility. *Clim Chang 2013 Phys Sci Basis Contrib Work Gr I to Fifth Assess Rep Intergov Panel Clim Chang*:1029–1136.
7. Sherwood SC, Huber M (2010) An adaptability limit to climate change due to heat stress. *Proc Natl Acad Sci USA* 107(21): 9552-9555.
8. Steadman RG (1979) The Assessment of Sultriness. Part I: A Temperature-Humidity Index Based on Human Physiology and Clothing Science. *J Appl Meteorol* 18(7):861–873.
9. Fischer EM, Schär C (2010) Consistent geographical patterns of changes in high-impact European heatwaves. *Nat Geosci* 3(6):398–403.
10. Diffenbaugh NS, Pal JS, Giorgi F, Gao X (2007) Heat stress intensification in the Mediterranean climate change hotspot. *Geophys Res Lett* 34(11).
11. Iran city hits suffocating heat index of 165 degrees, near world record - The Washington Post Available at: https://www.washingtonpost.com/news/capital-weather-gang/wp/2015/07/30/iran-city-hits-suffocating-heat-index-of-154-degrees-near-world-record/ [Accessed August 18, 2016].
12. Guha-Sapir D, Below R, Hoyois P (2016) EM-DAT: The CRED/OFDA International Disaster Database– Université Catholique de Louvain Brussels – Belgium. Available at: www.emdat.be.
13. Fischer EM, Oleson KW, Lawrence DM (2012) Contrasting urban and rural heat stress responses to climate change. *Geophys Res Lett* 39(3).
14. Taylor KE, Stouffer RJ, Meehl GA (2012) An Overview of CMIP5 and the Experiment Design. *Bull Am Meteorol Soc* 93(4):485–498.
15. Kjellstrom T (2016) Impact of Climate Conditions on Occupational Health and Related Economic Losses: A New Feature of Global and Urban Health in the Context of Climate Change. *Asia Pac J Public Health* 28(2 Suppl):28S–37S.
16. Zhao Y, Ducharne A, Sultan B, Braconnot P, Vautard R (2015) Estimating heat stress from climate-based indicators: present-day biases and future spreads in the CMIP5 global climate model ensemble. *Environ Res Lett* 10(8):84013.
17. Pal JS, Eltahir EAB (2015) Future temperature in southwest Asia projected to exceed a threshold for human adaptability. *Nat Clim Chang* 6(2):197–200.
18. Smith J, et al. (2009) Assessing dangerous climate change through an update of the Intergovernmental Panel on Climate Change (IPCC) "reasons for concern." *Proc Natl Acad Sci USA* 106(11):4133–4137.
19. Diffenbaugh NS, Scherer M (2011) Observational and model evidence of global emergence of permanent, unprecedented heat in the 20th and 21st centuries. *Clim Change* 107(3):615–624.
20. Rogelj J, et al. (2016) Paris Agreement climate proposals need a boost to keep warming well below 2 °C. *Nature* 534(7609):631–639.
21. Hinkel J, et al (2013) Coastal flood damage and adaptation costs under 21st century sea-level rise. 15(9):3292-3287.
22. Frieler K, et al. (2012) Limiting global warming to 2 °C is unlikely to save most coral reefs. *Nat Clim Chang* 2(9):165–170.
23. Seneviratne SI, Donat MG, Pitman AJ, Knutti R, Wilby RL (2016) Allowable CO2 emissions based on regional and impact-related climate targets. *Nature* 529(7587):477–483.
24. Ford JD, et al. (2010) Case study and analogue methodologies in climate change vulnerability research. *Wiley Interdiscip Rev Clim Chang* 1(3):374–392.
25. Glantz MH (1991) The use of analogies in forecasting ecological and societal responses to global warming. *Environment* 33(5):11-33.
26. Knutti R, Rogelj J, Sedláček J, Fischer EM (2015) A scientific critique of the two-degree climate change target. *Nat Geosci* 9(1):13–18.
27. van der Linden S (2014) The social-psychological determinants of climate change risk perceptions: Towards a comprehensive model. *J Environ Psychol* 41:112–124.
28. Sterman JD (2011) Communicating climate change risks in a skeptical world. *Clim Change* 108(4):811–826.
29. Ballester J, Robine J-M, Herrmann FR, Rodó X (2011) Long-term projections and acclimatization scenarios of temperature-related mortality in Europe. *Nat Commun* 2.
30. Kolkata: Heat claims two more, toll reaches 18 | The Indian Express Available at: http://indianexpress.com/article/cities/kolkata/kolkata-heat-claims-two-more-toll-reaches-18/ [Accessed August 26, 2016].
31. India heatwave kills more than 500 people | World news | The Guardian Available at: https://www.theguardian.com/world/2015/may/25/india-heatwave-deaths-heatstroke-temperatures [Accessed August 26, 2016].
32. Hoornweg D, Pope K (2016) Population predictions for the worlds largest cities in the 21st century. *Environ Urban*.Online Sept, 2016. doi: 10.1177/0956247816663557.
33. O'Neill BC, et al. (2014) A new scenario framework for climate change research: The concept of shared socioeconomic pathways. *Clim Change* 122(3):387–400.
34. Stone B (2012) *The city and the coming climate: Climate change in the places we live* (Cambridge University Press, New York).
35. Oleson KW, et al. (2015) Interactions between urbanization, heat stress, and climate change. *Clim Change* 129(3–4):525–541.
36. Reckien D, et al. (2014) Climate change response in Europe: What's the reality? Analysis of adaptation and mitigation plans from 200 urban areas in 11 countries. *Clim Change* 122(1–2):331–340.
37. Knowlton K, et al. (2014) Development and implementation of South Asia's first heat-health action plan in Ahmedabad (Gujarat, India). *Int J Environ Res Public Health* 11(4):3473–92.
38. Brooke Anderson G, Bell ML, Peng RD (2013) Methods to calculate the heat index as an exposure metric in environmental health research. *Environ Health Perspect* 121(10):1111–1119.
39. Weedon GP, et al. (2014) The WFDEI meteorological forcing data set: WATCH Forcing Data methodology applied to ERA-Interim reanalysis data. *Water Resour Res* 50(9):7505–7514.
40. Dee DP, et al. (2011) The ERA-Interim reanalysis: configuration and performance of the data assimilation system. *Q J R Meteorol Soc* 137(656):553–597.
41. Morice CP, Kennedy JJ, Rayner NA, Jones PD (2012) Quantifying uncertainties in global and regional temperature change using an ensemble of observational estimates: The HadCRUT4 data set. *J Geophys Res Atmos* 117(D8).
42. Rohde R, et al. (2013) A new estimate of the average Earth surface land temperature spanning 1753 to 2011. *Geoinformatics Geostatistics An Overv* 1(1):1-7.
43. Hansen J, Ruedy R, Sato M, Lo K (2010) Global surface temperature change. *Rev Geophys* 48(4).
44. United Nations, Department of Economic and Social Affairs PD (2014) World Urbanization Prospects: The 2014 Revision, CD-ROM Edition.
45. Rye CJ, Arnold NS, Willis IC, Kohler J (2010) Modeling the surface mass balance of a high Arctic glacier using the ERA-40 reanalysis. *J Geophys Res Earth Surf* 115(F2).
46. Matthews T, Hodgkins R, Guðmundsson S, Pálsson F, Björnsson H (2015) Inter-decadal variability in potential glacier surface melt energy at Vestari Hagafellsjökull (Langjökull, Iceland) and the role of synoptic circulation. *Int J Climatol* 35(10):3041–3057.

Submitted PDF